Title: A multi-technique characterization of the stability of surfactant containing solid dispersion based buccal patches prepared by hot melt injection moulding

Authors: Muqdad Alhijjaj, Peter Belton, Sheng Qi

PII: S0378-5173(17)30556-2
DOI: http://dx.doi.org/doi:10.1016/j.ijpharm.2017.06.048
Reference: IJP 16772

To appear in: *International Journal of Pharmaceutics*

Received date: 3-5-2017
Revised date: 12-6-2017
Accepted date: 13-6-2017

Please cite this article as: Alhijjaj, Muqdad, Belton, Peter, Qi, Sheng, A multi-technique characterization of the stability of surfactant containing solid dispersion based buccal patches prepared by hot melt injection moulding.International Journal of Pharmaceutics http://dx.doi.org/10.1016/j.ijpharm.2017.06.048

A multi-technique characterization of the stability of surfactant containing solid dispersion based buccal patches prepared by hot melt injection moulding

Muqdad Alhijjaj[1,2], Peter Belton[3], and Sheng Qi[1*]

1. *School of Pharmacy, University of East Anglia, Norwich, Norfolk, UK, NR4 7TJ*
2. *Department of Pharmaceutics, College of Pharmacy, University of Basrah, Basrah, Iraq*
3. *School of Chemistry, University of East Anglia, Norwich, Norfolk, UK, NR4 7TJ*

Correspondence: Sheng Qi, sheng.qi@uea.ac.uk; Fax number: +44 1603592023

Graphical abstract

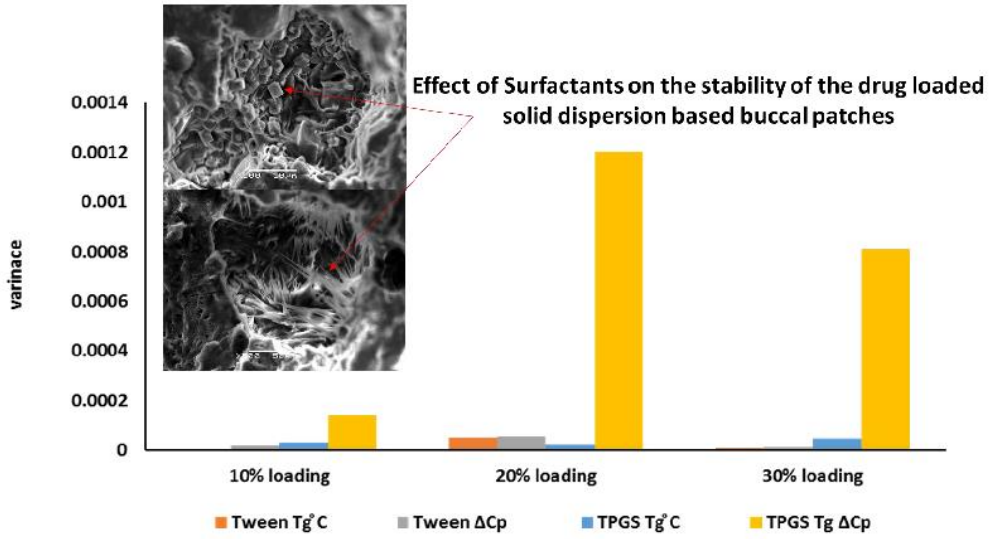

Abstract

This study investigates the stability of typically complex multi-component hydrophilic solid dispersions that could be used in a clinical application. Felodipine solid dispersions in two types of blends consisting of PEG, PEO and Tween 80 or Vit E TPGS were prepared by hot melt-injection moulding (HMIM) across a range of drug loadings and subjected to a range of storage conditions. Microscopy, thermal analysis, spectroscopy and powder X-ray diffraction were used to characterize the systems. The semi-solid surfactant TPGS showed a better solubilizing effect on the drug than the liquid surfactant Tween 80 in the fresh state and offered some degree of protection over the chemical degradation of PEG/PEO. Better storage stability was observed for the systems with low drug loading. Crystallization of a new metastable polymorphic form of felodipine in the patches with drug loadings at and above the saturation point was observed. Quantitative comparison of the data sets was achieved by a normalisation process and calculation of statistical variance. TPGS containing patches were more sensitive to the aging process than Tween containing patches. For both surfactants, such instability is

more responsive to the storage temperature than humidity. This study established a methodology for probing the complex stabilities of multi-component dispersions.

Keywords:

Hot melt extrusion, injection moulding, surfactants, solid dispersions, physical stability, polymorph

Introduction

Surfactants, such as Tween 80 and TPGS, have been suggested for use as plasticizers in hot melt extruded solid dispersions to ease the extrusion process (Ghebremeskel et al., 2007; Goddeeris et al., 2008; Morris et al., 1992; Repka and McGinity, 2000, 2001). Recently it has also been reported that the addition of significant amount of surfactant can also improve the solubility of drugs in the matrix by creating phase separated surfactant rich drug compartments in which the drug is soluble (Alhijjaj et al., 2015; Alhijjaj et al., 2016). In some cases, the surfactants have been reported to be responsible for destabilizing the drug and cause crystallization of drug from the dispersions during storage (Galop, 2005; Ghebremeskel et al., 2006; Janssens et al., 2008; Wang et al., 2005). The mechanism of this destabilizing effect has been mainly attributed to the low T_g of such materials (Ghebremeskel et al., 2006; Janssens et al., 2008; Mosquera-Giraldo et al., 2014). However, the guidance for surfactant selection and control such destabilizing effects have been not fully developed. This study aims to contribute to a fuller understanding of the destabilization effect of the use of surfactants in hot melt

extruded formulations by investigating the stability of two types surfactant-containing hot-melt injection moulded (HMIM) patches.

Whilst simple binary model systems can be of great value in understanding basic principles of stabilities of solid dispersions, practical formulations used in real clinical applications are often multi-component systems. It is clear that the likely behaviour of a clinically realistic formulation is going to be complicated. Therefore, this study systematically investigates such systems in order to be in a better position to predict how actual practical formulations will behave. The multi-component dispersion based patches described here are prepared using low temperature and single step processing without the use of organic solvents. They are mucoadhesive and could be applied clinically as buccal patches for improving the bioavailability of felodipine by bypassing hepatic metabolism which can remove up to 84% of the administered dose (Edgar et al., 1985). The formulations contained a mixture of polyethylene glycol (PEG), polyethylene oxide (PEO) and Tween 80 or D-α–tocopheryl polyethylene glycol 100 succinate (TPGS) in the ratio 4:3:3. This ratio was kept constant with felodipine loadings of 10, 20 and 30% w/w. The patches containing PEG/PEO and Tween 80 were abbreviated as CM1 while the ones containing PEG/PEO and TPGS were abbreviated as CM2. Previously the co-existences of multiple phases were identified in these multi-component patches (Alhijjaj et al., 2015; Alhijjaj et al., 2016). These phases are a surfactant rich phase containing drug and crystalline and amorphous polymer, amorphous and crystalline polymer phase which may also contain some surfactant and drug. The relationships between the phases are likely to change on storage as a result of the tendency to move to an equilibrium condition with time and the effects of temperature and humidity. If the drug is heterogeneously distributed at a microscopic level (Alhijjaj et al., 2015; Alhijjaj et al., 2016) there could be multiple drug crystallisation mechanisms which could result in polymorphic forms of the drug.

In addition, the stability of each excipient may also impact on the overall stability of the formulations. For example, the crystalline PEG/PEO phase can exist in more than one crystalline form: a folded form and a linear form (Buckley and Kovacs, 1976; Craig, 1995). Changes of PEG/PEO from a less folded form to folded form on aging could be the secondary cause of drug instability as changes in crystallinity and crystal thickening on storage have been reported in literature (Bley et al., 2010; Damian et al., 2002; Dordunoo et al., 1997; Duong et al., 2015; Papageorgiou et al., 2006; Weuts et al., 2005). Taking into consideration of all the variables, this study first investigated the effects of the surfactants on the stability of the multi-component drug-free carrier systems. The impacts of drug incorporation on the stability of the carrier were then analyzed. Finally the effects of surfactants on the drug recrystallization were studied. The three streams of data with the use of data normalisation and variance analyses of the high quantity of thermal data allowed the analysis of the interconnected relationship between the stability of the excipients and the stability of the drug in a semi-crystalline multi-component dispersion.

Materials and methods

Materials

The model drug, felodipine, was purchased from Afine Chemicals Ltd (Hangzhou, China). Polysorbate (Tween® 80) with a molecular weight of 1310 g/mole and phosphorus pentoxide (P_2O_5) with a purity of 99% were purchased from Sigma-Aldrich (Dorset, UK). Polyethylene glycol (PEG) 4000 with an average molecular weight of 4060 g/mole was supplied from Sigma-Aldrich (Poole, UK). Polyethylene oxide (PEO) WSR 1105 with an average molecular weight of 900,000 g/mole was kindly donated by Colorcon Ltd (Dartford, UK). Vitamin E TPGS with a molecular weight of 1513 g/mole was kindly donated by BASF (Ludwigshafen, Germany). NaCl (≥ 99.0 %) was purchased from Thermo Fisher Scientific (Geel, Belgium).

Preparation of placebo and felodipine loaded HMIM patches

A co-rotating twin screw bench-top hot melt extruder (HAAK MiniLab II Micro Compounder, Thermo Electron, Karlsruhe, Germany) with an injection moulding apparatus (HAAKE MiniJet System, Thermo Electron Corporation, Karlsruhe, Germany) was used in the fabrications of placebo and felodipine loaded solid dispersions. The injection mould allowed the production of patches with a final geometry of 25 mm × 25 mm × 0.5 mm. Two sets of formulations containing either Tween 80 (abbreviated as CM1) or TPGS (abbreviated as CM2) were prepared. Placebos and patches with 10, 20 and 30% w/w drug loadings were formulated with the PEG/PEO/surfactant weight ratios of 40/30/30, 36/27/27, 32/24/24 and 28/21/21, respectively. Before extrusion, physical mixtures of the formulations were prepared at different drug loadings by initially mixing of crystalline felodipine with either liquid Tween 80 or the molten TPGS (65 °C) followed by the addition of the other excipients and all the components of formulations were mixed thoroughly using a mortar and pestle for at least 2 minutes at room temperature. These mixtures were then fed into the extruder operating at a barrel temperature of 65 °C and a screw rotation of 100 rpm with 5 minutes of residence time. After extrusion, the extruded soft masses were loaded into the pre-heated cylinder of the injection moulding apparatus (65 °C). The materials were injected into the patch pre-heated mould (65 °C) under 300 bars pressure for 20 seconds. The patches were collected after being cooled inside the mould for 1 hour at ambient temperature.

Storage conditions of the dispersion patches

After preparation, the placebo and drug loaded patches were immediately stored in four different conditions for 3-month stability testing. The four conditions are abbreviated as A, B, C and D conditions and they refer to room temperature with 0% relative humidity (RH), room

temperature with 75% RH, 40 ºC with 0% RH, and 40 ºC with 75% RH, respectively. Storage containers containing phosphorus pentoxide (P_2O_5) were used to represent the 0% RH. Supersaturated NaCl solution was used to provide the 75% RH. A stability incubator (Genlab incubator, Genlab Ltd, Cheshire, UK) was used to provide the 40℃ condition. All samples were stored for 3 months and tested periodically.

Characterization of HMIM aged solid dispersions

Scanning Electron Microscopy (SEM)

For the purpose of comparison, fresh and aged samples at different conditions were scanned using JSM 5900LV Field Emission Scanning Electron Microscope (Jeol Ltd, Japan) equipped with a tungsten hairpin electron gun. Surfaces and cross sections (prepared by cutting the samples after dipping into liquid nitrogen) of all samples were investigated for the presence or absence of crystal growth and changes in the microstructure of the matrices. The scanned samples were coated with gold using a Polaron SC7640 sputter gold coater (Quorum Technologies, Newhaven, UK) prior to imaging.

Energy-Dispersive X-ray Spectroscopy (EDS)

In order to confirm the chemical identity of the detected crystal growth, the presence of the two chlorine atoms in the structure of felodipine were used as a chemical marker for the identification of drug crystals. EDS (INCA Energy manufactured by Oxford Instruments) combined with SEM was used. The analyses were conducted using single point X-ray acquisition mode with at least 3 points were analyzed for each morphological feature (crystals, matrix surface, matrix cross section) in the scanned area ≈ 0.5 x 0.5 cm^2 of the sample. The acquisition time was 30 seconds with electron acceleration voltage was 20 kV.

Powder X-Ray Diffraction (PXRD)

The diffraction patterns of the fresh and the aged samples were analyzed using Thermo ARL Xtra X-ray diffractometer (Thermo Scientific, Switzerland) equipped with a copper X-ray Tube (λ =1.540562 Å). An X-ray beams with a voltage of 45 kV and a current of 40 mA. The angular scan range was ($5^\circ < 2\Theta < 60^\circ$) using a step-scan mode with step width of 0.01˚ and scan speed of 1 sec/step were used to acquire the diffraction patterns.

Attenuated Total Reflectance Fourier Transform Infrared Spectroscopy (ATR-FTIR)

All samples were scanned using an IFS 66/S FTIR spectrometer (Bruker Optics Ltd, Coventry, UK) fitted with a Golden Gate® ATR accessory. The acquired ATR-FTIR spectra, in absorbance mode, were obtained using a scanning resolution of 2 cm^{-1} and 32 scans for each sample. Three replicate were performed for each formulation.

Differential Scanning Calorimetry (DSC)

A Q-2000 MTDSC (TA Instruments, Newcastle, USA) equipped with a RC90 cooling unit was used to analyze the placebo and felodipine loaded patches. A scanning rate of 10 ºC/min was used for all samples. The DSC was fully calibrated prior to the sample measurements. Three replicates of 2-3 mg of each sample taken randomly were analyzed using standard Aluminum TA crimped pans (TA Instruments, Newcastle, USA). Universal Analysis software was used to analyze the collected thermograms.

Thermogravimetric Analysis (TGA)

In order to estimate the loss of moisture content and thermal degradation profiles of the samples, raw materials, placebos and drug-loaded solid dispersions were analyzed using TGA Q5000 (TA Instruments, Newcastle, USA). A heating rate of 10 ºC/min was used for all

samples. Each sample was tested in triplicate. Universal Analysis software was used to analyze the acquired results.

Statistical Analysis

The results obtained using EDS and DSC were statistically analyzed using one-way analysis of variance (ANOVA). Differences of $p < 0.05$ were considered to be significant.

Results

Effects of the surfactants on the stabilities of semi-crystalline carriers in the placebo patches

CM1 contains a liquid (at ambient temperature) surfactant, Tween 80 and CM2 contains a solid surfactant, TPGS. The addition of surfactant to the semi-crystalline mixture of PEG and PEO resulted in the formation of an extra phase. As seen in Figure 1, in the fresh placebos both Tween and TPGS were phase separated as indicated by their detectable endothermic melting peaks (as peak temperature) at -10.3 ± 0.2 and 37.5 ± 0.1 °C, respectively. When PEG and PEO were extruded without the surfactants at the ratio of 4:3 (w/w), which is the ratio used in the patches, a single melting with a peak temperature of 69.5 ± 1.5 °C (Supplementary Material Figure S1) was observed. As seen in Figure 1, the DSC results of the placebo patches also show single melting transitions lower than the melting of PEG/PEO extrudates at 63.6 ± 0.2 °C and 64.1 ± 0.3 °C for CM1 and CM2, respectively. The depressions of PEG/PEO melting temperature may indicate some degree of miscibility between the surfactants and the polymers. However, the melting enthalpy values of the fresh surfactant-containing placebo patches (178.96 ± 0.60 J/g for fresh CM1 and 178.10 ± 3.01 J/g for fresh CM2) are significantly higher than the enthalpy values of the pure PEG/PEO extrudates (154.30 ± 5.83 J/g). This could be due to the formation of the folded form of the metastable folded polymorphs of PEG and PEO that have lower melting points and have been reported to be induced by additives to PEG and

PEO (Dordunoo et al., 1997; Verheyen et al., 2001).

After 3-month aging, no morphological change was observed except CM1 patches liquefied under condition D. TGA results of the CM1 placebo stored under condition D show continuously weight loss from 20 °C (Figure 2A), whereas the samples stored at other aging conditions only show significant weigh loss at the thermal decomposition temperatures of the excipients around 370 °C (Figure 2B). The gradual weight loss at low temperatures may be attributed to the loss of low molecular weight degradation products during heating. Tween and PEG/PEO have been reported to go through thermally initiated autoxidation in literature (Ha et al., 2002; Han et al., 1995; Kerwin, 2008; Kishore et al., 2011; Lai and Liau, 2003). The presence of high humidity and temperature (as condition D) could accelerate this degradation process and generate a range of degradation products. The DSC results of the aged CM1 placebos indicate no changes of the patches aged under condition A, B and C. However, no PEG/PEO melting was detected in the patches aged under condition D (Figure 1A). This again supported the hypothesis of degradation of CM1 placebo under condition D.

Similar to the aged CM1 placebos, the DSC results indicate good stability of CM2 placebo under conditions A, B and C (Figure 1B). For CM2 patches aged under condition D, two additional shoulder peaks at 55 °C and 59.5 °C can be observed for PEG/PEO melting which may be attributed to a small extent of degradation of PEG/PEO. There are no changes in the melting behaviour of the TPGS phase. This result indicates that TPGS has better protective effect of the polymers from degradation during aging under high humidity and temperature.

Effect of drug loading on the semi-crystalline carriers in fresh state

After assessing the effect of the surfactant on the polymer, the effects of the incorporation of

drug on the surfactant-polymer carriers were investigated. The comparisons of the morphologies of the surfaces and cross-sections of the placebos and drug-loaded patches are shown in Figure 3. Drug loading leads to increased surface roughness of the fresh CM1 patches. The DSC results of the drug loaded CM1 samples show no melting of Tween. A shoulder at the onset of the melting of PEG/PEO developed with increasing the drug loading to 20 and 30% (Figure 4 A and C). At 30% drug loading, a separate melting peak at 87 °C can be detected. This is assigned to the significantly depressed melting of crystalline felodipine, indicating of the presence of crystalline felodipine in CM1 patches with 30% drug loading CM1 patches. Single T_g's were detected for all drug loaded fresh CM1 patches (at -49.0 ± 0.6, -38.0 ± 0.3 and -46.6 ± 0.5 °C for 10, 20 and 30% drug loading, respectively). These T_gs are higher than the T_g of both Tween and PEG/PEO, but lower than the T_g of amorphous felodipine. Therefore, it is reasonable to assign these T_g to the amorphous phase containing Tween, drug and PEO/PEG. The decrease of T_g in fresh 30% CM1 indicates a smaller amount of drug in the amorphous phase and is consistent with the observed melting of crystalline drug in the samples. Interestingly, no melting of Tween 80 was detected in all fresh CM1 patches with 10-30% drug loading, whereas the melting of the phase separate Tween 80 phase can be clearly observed in the fresh CM1 placebo patches. This suggests that the incorporation of the drug disrupted the crystallization of Tween possibly due to the dissolution of drug in the Tween phase.

The drug loaded fresh CM2 patches show the separate melting of the TPGS phase at 28.9 ± 0.3, 20.4 ± 0.4 and 24.9 ± 1.5 °C for 10, 20, and 30% drug loaded systems, respectively. These melting are significantly lower than the melting of pure TPGS (37.2 ± 0.2 ℃) and the melting of the TPGS phase in the placebo patches. This indicates that certain amount of the drug was solubilized in the TPGS phase, which caused the significant depression of the TPGS melting compared to the pure TPGS. Assuming the lowering of melting point is an indicator of drug

solubility, it is clear that the 20% drug loaded system had more drug dissolved in the TPGS than 10 and 30% loaded systems. In contrast to CM1, no melting of felodipine is seen in the DSC results of the 30% drug-loaded CM2 samples. Despite there is the possibility of the dissolution of crystalline felodipine on heating during the DSC experiment, it is still valid to suggest based on this evidence that TPGS shows better drug solubilization/stabilization effect than Tween 20 in the fresh state. This is in good agreement with the PXRD data of the fresh samples. Lower level of crystalline drug was detected in patches with 10-30% loading indicates that CM2 is better at initially solubilizing felodipine than CM1.

Carrier stability of drug loaded patches aged under 0%RH (conditions A and C)

Two key thermal transition regions in the DSC results of the drug-loaded patches on aging were monitored, the T_g and the melting regions. As summarized in Table 1, for 10% drug loaded CM1 and CM2 patches stored under condition A, little changes were observed for the surfactant related thermal transitions. Being stored at 40 °C (condition C) resulted in the appearance of the phase separate Tween melting transition and increased TPGS melting point and enthalpy values. More changes in the PEG/PEO phases (increases in the melting points and enthalpy values) were identified in aged CM1 patches than CM2 patches for both condition A and C. These results indicate that even at 10% drug loading aged CM1 patches already showed more signs of phase separation of the surfactant and instability of the polymers than CM2 patches. The results also highlighted the influence of temperature on these instabilities.

For the aged CM1 and CM2 patches with 20 and 30% drug loadings, both T_g and associated ΔC_p values decreased. As discussed above, the single T_gs of the patches are indications of a mixed amorphous phase of carrier and the drug as the T_gs are higher than the T_g of the carrier and lower than the T_g of the amorphous drug. As the drug behaves as an anti-plasticizer, the

decreases in T_g values after aging are an indication of a reduction in amount of amorphous drug in the carrier rich phases. In addition, melting of Tween 80 was detected in 20% CM1 stored under 40 ºC and 30% CM1 stored under both room temperature and 40 ºC. For CM2 patches, the melting point and enthalpy values of the TPGS phases were increased for both condition A and C. For both CM1 and CM2, the changes are greater for patches with 20% drug loading than the 30% samples. We discuss the implications of this observation in the section below concerning drug crystallization phenomena.

New shoulder peaks (as highlighted by •) close to the offset regions of PEG/PEO melting of the 20% CM1 and CM2 samples stored at condition C were observed (Figure 4 A and C). As discussed earlier for the fresh 30% drug loaded CM1, these peaks are attributed to recrystallized drug into the aged samples. These crystalline drug related peaks are absent in the aged 30% drug loaded CM2 under both conditions A and C.

For the aged 20 and 30% CM1 samples, the melting transitions of Tween (absent in fresh sample) are detectable indicating Tween 80 phase separation except the 20% aged patches at condition A. Tween 80 melting peaks were also undetectable for 10% CM1 samples stored at condition A. This indicates that higher storage temperature promotes the phase separation of the drug from the surfactant phase, which subsequently led to the detected melting of the crystallized Tween 80.

For the aged CM2 patches, the melting peaks of TPGS phases shift to a higher temperatures which are closer to the melting point of pure TPGS (Figure 4 C and G) and show increased enthalpy of melting values (Table 1). This indicates more complete phase separation of TPGS which may also be due to the crystallization of drug from TPGS phase. The increase in the

melting temperature and the enthalpy of melting of the TPGS in the 30% drug-loaded patches is greater than that of the 20% drug-loaded patches. This implies more drug dissolved in the TPGS in the 20% sample than the 30% sample. It also should be mentioned that greater increases in the melting enthalpy values of the TPGS were seen in the DSC results of the 20 and 30% loaded CM2 patches aged at 40 °C than at room temperature (Supplementary materials Tables S1 and S2) which again indicates that higher storage temperature have more significant effect on the stability and the process of the phase separation of the solid dispersions. Once the surfactants are phase separated in their crystalline form, lower amounts of drug are solubilized in the surfactant phases. This suggests that more crystalline drug is likely to be present in 30% drug loaded samples under condition C, consistent with our previous observations.

Carrier stability of drug loaded patches under 75%RH (Condition B and D)

Under 75% RH, for 10% drug-loaded CM1 and CM2 little change was observed (Table 1) for the surfactants and PEG/PEO related thermal transitions. For 20-30% drug loaded CM1 and CM2, the common features are decreased T_g and ΔC_p values, accompanied by the increased melting enthalpy of the surfactant phases. The changes between conditions B and D are greater for CM2 than for CM1 indicating CM2 patches were more sensitive to humidity induced instability. This is further confirmed by the depressed melting of felodipine in aged CM2 patches that was detected under both conditions B and D and which were absent in the samples aged under 0%RH. This indicates that high humidity led to more drug crystallization in TPGS containing samples. For CM2, a more significant effect of storage temperature on the stability is also demonstrated by comparison of the differences between the melting enthalpy of TPGS for the aged patches under conditions A and C and conditions B and D (Supplementary materials Tables S1 and S2). The differences between A and C are greater than those between

A and B (in addition the differences between C and D are greater than those between B and D) suggesting that the storage temperature has more impact on the instability of CM2 patches. For all patches aged under condition D, the development of multiple peaks on the melting peak of PEG/PEO were observed (Figure 4). We assign these to the melting of degradation products of PEG/ PEO due to the random chain scission of the two polymers caused by oxidative thermal degradation.

Effect of surfactants on crystallisation tendency and crystal growth of felodipine on aging

Felodipine can crystallize in a range of polymorphs due to the flexibility of its molecular structure (Akune et al., 2015; Surov et al., 2012). Since the determination of felodipine form I crystal structure in 1986, several studies have been published reporting new polymorphic forms (II-IV) obtained from various solvents (Lou et al., 2009; Mishra et al., 2014; Rollinger and Burger, 2001; Srčič et al., 1992; Surov et al., 2012; Wang et al., 2015). This part of the study focuses on the felodipine crystallization in the aged samples. Using SEM in combination with EDS the crystal growth of felodipine on and in the patches were monitored. Table 2 summarizes the drug crystallization and crystal habits after 3 months aging under the 4 different conditions. Except for the 20% CM1 stored at condition C and 10% CM2 stored at condition D, drug recrystallization occurred during aging in all formulations. Generally, more drug crystallization was observed on the surface of the patches and the interior of the air pockets than the bulk matrix of the samples. This is likely to be due to the surface being the hydrophobic (air exposed) interface experiencing highest temperature and humidity at least at the initial few hours of the aging process. These results are consistent with data reported in literature revealing faster surface to bulk drug crystallization (Wu and Yu, 2006; Zhu et al., 2008). There are three main types of felodipine crystal habits observed, blocks, plates and needles arranged in a spherulitic pattern (Figure 5). In literature the crystal habits of the polymorphs were reported to be block

shaped for polymorphs I and II and plate-like crystals for form III (Surov et al., 2012), but no information about the crystal habit of polymorph IV of felodipine (Mishra et al., 2014) is available. In this study the spherulitic crystals were only observed in the interior or on the surface after aging under 40 °C (condition C and D). The blocks and plate crystals are more common than the needle crystals and they were observed on the surfaces and interior of most formulations.

In order to further identify the polymorphic form of the recrystallized felodipine, PXRD and ATR-FTIR were used to characterize the aged samples. Table 3 summarizes the identification of the polymorphs using PXRD and ATR-FTIR results. No PXRD detectable drug crystallization was observed in both 10% drug loaded CM1 and CM2 patches due to the low quantity of the crystalline materials. However, the observation of surface crystals for these samples by SEM (supplementary material Figure S2 and S3) may explain the detected presence of crystalline material in the ATR-FTIR spectra. As seen in Figure 6, the diffraction pattern of the aged 20% w/w CM1 patch under condition A indicates the presence of form I (Surov et al., 2012). This is consistent with the SEM results as form I is the usually present in the block shaped habit (Mishra et al., 2014). The presence of mixture of form I and II was indicated in the PXRD pattern of the 20% drug loaded CM1 sample stored under condition B. It should be mentioned that Figure 6 only shows the section of the PXRD diffraction patterns of the samples that contain the smallest number of interfiling polymer and surfactant peaks (13.6°, 14.5°, 15.1°, 17.2°, 18.4° and 19.1°). Under high storage temperature (condition C and D) new peaks at 9.3° and 12.4° are observed in the diffraction patterns of the aged patches. These diffraction peaks do not match with any known polymorphs of felodipine in the literature, suggesting the presence of an unknown new metastable polymorph. For 20% drug loaded CM2 samples, fewer recrystallization diffraction peaks with lower relative intensities were identified compared to

the corresponding CM1 loaded samples. This may again suggest the higher solubilization capacity and stabilization ability of TPGS containing CM2 matrices compared CM1 formulations. However, it is interesting to observe the diffraction peaks at 9.3°, and 12.4° in aged CM2 samples stored at all conditions. This indicates that the CM2 matrices promote the crystallization of the metastable new form.

For the 30% drug loaded samples (Figure 7), it is noted that form I felodipine is present in fresh CM1. The polymorph of the drug in the fresh CM2 was not identified due to weak diffraction peaks and broad IR peaks. The diffraction patterns of the aged 30% drug-loaded CM1 samples under all conditions indicate the coexistence of the new form and form I. However, it is noted that regardless of the humidity, room temperature storage resulted in the higher yield of the form I than the new form as indicated by the relative intensities of peaks at 9.3°(corresponding to the new form) and at 10.8°(corresponding to form I). For 30% w/w CM2 formulations, storing under 0% RH led to the crystallization of form I; whereas the sample stored under 75% RH led to the crystallization of the new metastable form. This is supported by the new NH stretching of the samples that is different from the NH peak of form I.

Figure 8 displays the NH stretching vibration in the IR spectra of the aged 20 and 30% drug loaded CM1 and CM2 patches. NH stretching peaks at 3339 cm^{-1}, 3372, 3334, 3370, 3329 cm^{-1} have been reported for the identification of the amorphous and four crystalline polymorphic forms I-IV, respectively (Konno and Taylor, 2006; Lou et al., 2009; Rollinger and Burger, 2001; Srčič et al., 1992; Tang et al., 2002; Wang et al., 2015). Whilst other peaks do vary with form, these are the clearest and have least interference from the matrix peaks (Konno and Taylor, 2006; Tang et al., 2002). The spectra must be used with caution as the sample size is less than the total size of the patch and where crystals are formed they are necessarily regions

of inhomogeneity with a drug rich region adjacent to drug poor regions. In the case of limited surface crystallisation this situation is exacerbated. Since in ATR-FTIR the penetration of the evanescent wave is of the order of micron crystals at the surface will be preferentially sampled (Campbell, 2012). This can result in the appearance of apparently high concentrations of the crystalline forms and explains the observations of a signal from crystals in the 10% samples where none were observed in PXRD. Using these signature peaks, it is possible to confirm the identification of the polymorphic forms detected by PXRD. CM1 samples stored at condition C and D and CM2 samples stored at all conditions revealed an new NH stretching peak at 3321 cm^{-1} which is not related any known polymorphs or the amorphous form. As the PXRD results indicated that the growth of the new form is favoured at 40℃, it is reasonable to suggest that the NH stretching peak at 3321 cm^{-1} is a possible signature peak for a new polymorphic crystal form of felodipine. The ATR-FTIR results (Figure 8) show good agreement with PXRD data.

In summary it is clear that the growth of the new polymorphic form is favoured by TPGS containing dispersions when the drug loading is close to saturation (20% loading). When form I is already present in the fresh samples, the growth of the new form is more favoured by higher storage temperature but is not sensitive to humidity.

Discussion

This study investigated the stability of multi-component solid dispersions. Some inconsistencies of SEM, PXRD and IR results were observed. These are likely to be caused by the effect of sampling on the results obtained by different characterisation methods (Grisedale et al., 2011). Nevertheless from the data, two general observations can be summarized. 1) For both 0% and 75% RH, it is clear that storage at 40 °C led to a greater degree of phase separation than storage at room temperature. The observation that temperature had a greater effect on

stability than humidity suggests that key factor may be molecular mobility which is enhanced more by higher temperatures than water absorption. Another possibility is that the phase diagram for the system will be temperature dependent and the shift in phase relations could be due to changes in the relative solubilities with temperature. However we consider this is unlikely as the observed changes are of increased phase separation whereas the most likely effect of temperature on phase relations is to increase solubility. 2) For both CM1 and CM2, drug loading has significant impact on the aging behavior of the carrier materials. The CM1 and CM2 patches with 20% drug loading, which is at the boundary of the saturation point saturation of drug solubility in the carrier materials, showed the highest drug phase separation activity of the patches on aging. The patches with drug loadings below and above the saturation point showed less phase separation highlighting the important relationship between the degree of saturation and stability.

In order to make a more quantitative comparison of the changes observed the following process as used: normalisation was conducted by dividing the value of each thermal parameter for a given transition (e.g. Tween T_g or TPGS ΔH_f) by the sum of all the values for that transition across all storage conditions and drug loadings (including zero drug loading) during the 3-month aging period. This ensured the values across all the sets had the same order of magnitude so that changes were much easier to compare. Within particular data sets changes were quantified by calculating the statistical variance within the set. Normalized values of ΔC_p values and ΔH_f for TPGS and Tween are shown in Figure 9. ΔC_p is a measure of the amount of amorphous material thus the variation of ΔC_p during ageing represents changes in the amount of amorphous materials in the samples. As seen in Figure 9a, CM2 samples show a greater difference in ΔC_p between fresh and aged samples than CM1 samples. After aging, significant reductions in ΔC_p TPGS indicate the decreases in the amorphous TPGS contents in particular

for 20 and 30% drug loaded samples. The ΔH_f data of the aged CM2 samples in Figure 9b show increases after aging indicating increased phase separation of crystalline TPGS.

The smaller fluctuations in the ΔC_p values of the fresh and aged Tween samples for all drug loadings in comparison to the TPGS samples indicates a smaller change in the amount of amorphous Tween in the fresh and aged samples. The ΔH_f data of the Tween samples revealed that more crystalline Tween is generated after aging for most of the samples. The amount of the crystalline Tween increases with increasing the drug loading. Whilst generally increases in ΔC_p correspond to decreases in ΔH_f representing the transfer of material from an amorphous mixed phase to a single component phase the correlation is variable. This may be the effect of the variability of the amounts of dissolved drug in the amorphous phase causing changes in the intrinsic change in heat capacity at the glass transition

In order to further analyze the effect of storage, the variance of the set of parameters were calculated across the set of storage conditions for each drug loading. This gives direct measure of the size of the effect of storage condition. Figure 10a summarizes the influence of the surfactants on the thermal behaviour of PEG/PEO and highlights that TPGS has a stronger effect on the PEG/PEO behaviour of the aged formulations than Tween 80. Figure 10b demonstrates that the aging effects on TPGS thermal behaviour in CM2 is greater than that of Tween in CM1. In particular, more profound changes of the 20% loaded CM2 samples on aging demonstrated the importance of the relationship between drug-carrier solubility and stability. Boundary solubility should be avoided to minimize the instability associated with drug recrystallization. As seen in Figure 10a, the variances in PEG/PEO thermal behaviour during the aging period under all conditions are very much less than the ones observed for the thermal data of the surfactants. This indicates that the aging affects the stability of the surfactant phase

more than the PEG/PEO phase. If the surfactants and PEG/PEO are well mixed, this would not be case. Therefore this result suggests that in both CM1 and CM2 formulations the surfactants are largely phase separate from the PEG/PEO phase. However the scale of phases could not be concluded from the data of this study.

In addition, the chemical stability of the PEG/PEO based carrier material should also be carefully considered during formulation. In comparison to Tween containing CM1 samples, TPGS containing CM2 samples is much less vulnerable to degradation owing to the antioxidant activity of TPGS (Brouwers et al., 2006; Cagno et al., 2012; Carini et al., 1990; Crowley et al., 2002). For drug loaded CM1 patches, less signs of degradation of PEG/PEO were observed under high temperature and high humidity environments in comparison to placebos suggesting the drug incorporation also had protective effect to the carrier material from degradation, most likely to be antioxidation (Sugawara et al., 1996).

Conclusions

This study has investigated the effect of surfactants on the stability of multi-component dispersions which were intentionally formulated being phase separate. Semi-solid surfactant TPGS showed better stabilizing effect on the drug than the liquid surfactant Tween 80. The higher T_g and semi-solid nature of TPGS which provides higher viscosity in the dispersion are believed to contribute to its higher stabilising effect of the model drug. However, such stabilizing effect is only valid for the systems with drug loading below the saturation of drug in the carrier. With drug loading at the border and above the saturation, the stabilization advantage is significantly reduced. This correlation between the drug saturation level in the carrier materials and the overall formulation stability agrees well with literature data and can be applied to other solid dispersions in general. In addition, a new polymorphic form of

felodipine was observed in the aged samples. The crystallization of the new form is more sensitive to temperature than humidity and TPGS proved to be a good aid for the crystallization of the new form. We believe that the stability study methodology established in this study can be used in the studies of other multi-components solid dispersions systems.

Acknowledgement

Muqdad Alhjjaj would like to acknowledge the Higher Committee for Education Development in Iraq (HCED Iraq) for their generous financial support for his Ph.D and the European Interreg 2 Seas programme for supporing the project as a part of IMODE project.

References

Akune, Y., Gontani, H., Hirosawa, R., Koseki, A., Matsumoto, S., 2015. The effects of molecular flexibility and substituents on conformational polymorphism in a series of 2,5-diamino-3,6-dicyanopyrazine dyes with highly flexible groups. CrystEngComm 17, 5789-5800.

Alhijjaj, M., Bouman, J., Wellner, N., Belton, P., Qi, S., 2015. Creating Drug Solubilization Compartments via Phase Separation in Multicomponent Buccal Patches Prepared by Direct Hot Melt Extrusion–Injection Molding. Molecular Pharmaceutics 12, 4349-4362.

Alhijjaj, M., Yassin, S., Reading, M., Zeitler, J.A., Belton, P., Qi, S., 2016. Characterization of Heterogeneity and Spatial Distribution of Phases in Complex Solid Dispersions by Thermal Analysis by Structural Characterization and X-ray Micro Computed Tomography. Pharmaceutical Research, 1-19.

Bley, H., Fussnegger, B., Bodmeier, R., 2010. Characterization and stability of solid dispersions based on PEG/polymer blends. International Journal of Pharmaceutics 390, 165-173.

Brouwers, J., Tack, J., Lammert, F., Augustijns, P., 2006. Intraluminal drug and formulation behavior and integration in in vitro permeability estimation: A case study with amprenavir. Journal of Pharmaceutical Sciences 95, 372-383.

Buckley, C.P., Kovacs, A.J., 1976. Melting behaviour of low molecular weight poly (ethylene-oxide) fractions. Colloid and Polymer Science 254, 695-715.

Cagno, M.d., Stein, P.C., Styskala, J., Hlaváč, J., Skalko-Basnet, N., Bauer-Brandl, A., 2012. Overcoming instability and low solubility of new cytostatic compounds: A comparison of two approaches. European Journal of Pharmaceutics and Biopharmaceutics 80, 657-662.

Campbell, I., 2012. Biophysical Techniques. OUP Oxford.

Carini, R., Poli, G., Dianzani, M.U., Maddix, S.P., Slater, T.F., Cheeseman, K.H., 1990. Comparative evaluation of the antioxidant activity of α-tocopherol, α-tocopherol polyethylene glycol 1000 succinate and α-tocopherol succinate in isolated hepatocytes and liver microsomal suspensions. Biochemical Pharmacology 39, 1597-1601.

Craig, D.Q.M., 1995. Pharmaceuticals and Thermal AnalysisA review of thermal methods used for the analysis of the crystal form, solution thermodynamics and glass transition behaviour of polyethylene glycols. Thermochimica Acta 248, 189-203.

Crowley, M.M., Zhang, F., Koleng, J.J., McGinity, J.W., 2002. Stability of polyethylene oxide in matrix tablets prepared by hot-melt extrusion. Biomaterials 23, 4241-4248.

Damian, F., Blaton, N., Kinget, R., Van den Mooter, G., 2002. Physical stability of solid dispersions of the antiviral agent UC-781 with PEG 6000, Gelucire® 44/14 and PVP K30. International Journal of Pharmaceutics 244, 87-98.

Dordunoo, S.K., Ford, J.L., Rubinstein, M.H., 1997. Physical Stability of Solid Dispersions Containing Triamterene or Temazepam in Polyethylene Glycols. Journal of Pharmacy and Pharmacology 49, 390-396.

Duong, T.V., Van Humbeeck, J., Van den Mooter, G., 2015. Crystallization Kinetics of Indomethacin/Polyethylene Glycol Dispersions Containing High Drug Loadings. Molecular Pharmaceutics 12, 2493-2504.

Edgar, B., Regardh, C.G., Johnsson, G., Johansson, L., Lundborg, P., Lofberg, I., Ronn, O., 1985. Felodipine kinetics in healthy men. Clin Pharmacol Ther 38, 205-211.

Galop, M., 2005. Study of Pharmaceutical Solid Dispersions by Microthermal Analysis. Pharmaceutical Research 22, 293-302.

Ghebremeskel, A.N., Vemavarapu, C., Lodaya, M., 2006. Use of Surfactants as Plasticizers in Preparing Solid Dispersions of Poorly Soluble API: Stability Testing of Selected Solid Dispersions. Pharmaceutical Research 23, 1928-1936.

Ghebremeskel, A.N., Vemavarapu, C., Lodaya, M., 2007. Use of surfactants as plasticizers in preparing solid dispersions of poorly soluble API: Selection of polymer–surfactant combinations using solubility parameters and testing the processability. International Journal of Pharmaceutics 328, 119-129.

Goddeeris, C., Willems, T., Houthoofd, K., Martens, J.A., Van den Mooter, G., 2008. Dissolution enhancement of the anti-HIV drug UC 781 by formulation in a ternary solid dispersion with TPGS 1000 and Eudragit E100. European Journal of Pharmaceutics and Biopharmaceutics 70, 861-868.

Grisedale, L.C., Jamieson, M.J., Belton, P.S., Barker, S.A., M. Craig, D.Q., 2011. Characterization and quantification of amorphous material in milled and spray-dried salbutamol sulfate: A comparison of thermal, spectroscopic, and water vapor sorption approaches. Journal of Pharmaceutical Sciences 100, 3114-3129.

Ha, E., Wang, W., John Wang, Y., 2002. Peroxide formation in polysorbate 80 and protein stability. Journal of Pharmaceutical Sciences 91, 2252-2264.

Han, S., Kim, C., Kwon, D., 1995. Thermal degradation of poly(ethyleneglycol). Polymer Degradation and Stability 47, 203-208.

Janssens, S., Nagels, S., Armas, H.N.d., D'Autry, W., Van Schepdael, A., Van den Mooter, G., 2008. Formulation and characterization of ternary solid dispersions made up of Itraconazole and two excipients, TPGS 1000 and PVPVA 64, that were selected based on a supersaturation screening study. European Journal of Pharmaceutics and Biopharmaceutics 69, 158-166.

Kerwin, B.A., 2008. Polysorbates 20 and 80 Used in the Formulation of Protein Biotherapeutics: Structure and Degradation Pathways. Journal of Pharmaceutical Sciences 97, 2924-2935.

Kishore, R.S.K., Pappenberger, A., Dauphin, I.B., Ross, A., Buergi, B., Staempfli, A., Mahler, H.-C., 2011. Degradation of Polysorbates 20 and 80: Studies on Thermal Autoxidation and Hydrolysis. Journal of Pharmaceutical Sciences 100, 721-731.

Konno, H., Taylor, L.S., 2006. Influence of Different Polymers on the Crystallization Tendency of Molecularly Dispersed Amorphous Felodipine. Journal of Pharmaceutical Sciences 95, 2692-2705.

Lai, W.-C., Liau, W.-B., 2003. Thermo-oxidative degradation of poly(ethylene glycol)/poly(l-lactic acid) blends. Polymer 44, 8103-8109.

Lou, B., Boström, D., Velaga, S.P., 2009. Polymorph Control of Felodipine Form II in an Attempted Cocrystallization. Crystal Growth & Design 9, 1254-1257.

Mishra, M.K., Desiraju, G.R., Ramamurty, U., Bond, A.D., 2014. Studying Microstructure in Molecular Crystals With Nanoindentation: Intergrowth Polymorphism in Felodipine. Angewandte Chemie International Edition 53, 13102-13105.

Morris, K.R., Knipp, G.T., Serajuddin, A.T.M., 1992. Structural Properties of Polyethylene Glycol-Polysorbate 80 Mixture, a Solid Dispersion Vehicle. Journal of Pharmaceutical Sciences 81, 1185-1188.

Mosquera-Giraldo, L.I., Trasi, N.S., Taylor, L.S., 2014. Impact of surfactants on the crystal growth of amorphous celecoxib. International Journal of Pharmaceutics 461, 251-257.

Papageorgiou, G.Z., Bikiaris, D., Karavas, E., Politis, S., Docoslis, A., Park, Y., Stergiou, A., Georgarakis, E., 2006. Effect of physical state and particle size distribution on dissolution enhancement of nimodipine/PEG solid dispersions prepared by melt mixing and solvent evaporation. The AAPS Journal 8, E623-E631.

Repka, M.A., McGinity, J.W., 2000. Influence of Vitamin E TPGS on the properties of hydrophilic films produced by hot-melt extrusion. International Journal of Pharmaceutics 202, 63-70.

Repka, M.A., McGinity, J.W., 2001. Bioadhesive properties of hydroxypropylcellulose topical films produced by hot-melt extrusion. Journal of Controlled Release 70, 341-351.

Rollinger, J.M., Burger, A., 2001. Polymorphism of racemic felodipine and the unusual series of solid solutions in the binary system of its enantiomers. Journal of Pharmaceutical Sciences 90, 949-959.

Srčič, S., Kerč, J., Urleb, U., Zupančič, I., Lahajnar, G., Kofler, B., Šmid-Korbar, J., 1992. Investigation of felodipine polymorphism and its glassy state. International Journal of Pharmaceutics 87, 1-10.

Sugawara, H., Tobise, K., Kikuchi, K., 1996. Antioxidant Effects of Calcium Antagonists on Rat Myocardial Membrane Lipid Peroxidation. Hypertension Research 19, 223-228.

Surov, A.O., Solanko, K.A., Bond, A.D., Perlovich, G.L., Bauer-Brandl, A., 2012. Crystallization and Polymorphism of Felodipine. Crystal Growth & Design 12, 4022-4030.

Tang, X.C., Pikal, M.J., Taylor, L.S., 2002. A Spectroscopic Investigation of Hydrogen Bond Patterns in Crystalline and Amorphous Phases in Dihydropyridine Calcium Channel Blockers. Pharmaceutical Research 19, 477-483.

Verheyen, S., Augustijns, P., Kinget, R., Van den Mooter, G., 2001. Melting behavior of pure polyethylene glycol 6000 and polyethylene glycol 6000 in solid dispersions containing diazepam or temazepam: a DSC study. Thermochimica Acta 380, 153-164.

Wang, L., Song, Y., Yang, P., Tan, B., Zhang, H., Deng, Z., 2015. Preparation and thermodynamic properties of Felodipine form IV. Journal of Thermal Analysis and Calorimetry 120, 947-951.

Wang, X., Michoel, A., Van den Mooter, G., 2005. Solid state characteristics of ternary solid dispersions composed of PVP VA64, Myrj 52 and itraconazole. International Journal of Pharmaceutics 303, 54-61.

Weuts, I., Kempen, D., Verreck, G., Decorte, A., Heymans, K., Peeters, J., Brewster, M., Mooter, G.V.d., 2005. Study of the physicochemical properties and stability of solid dispersions of loperamide and PEG6000 prepared by spray drying. European Journal of Pharmaceutics and Biopharmaceutics 59, 119-126.

Wu, T., Yu, L., 2006. Surface Crystallization of Indomethacin Below T g. Pharmaceutical Research 23, 2350-2355.

Zhu, L., Wong, L., Yu, L., 2008. Surface-Enhanced Crystallization of Amorphous Nifedipine. Molecular Pharmaceutics 5, 921-926.

Figure 1. DSC thermograms of placebo (A) CM1 and (B) CM2 patches (with a scanning rate of 10℃/ min).

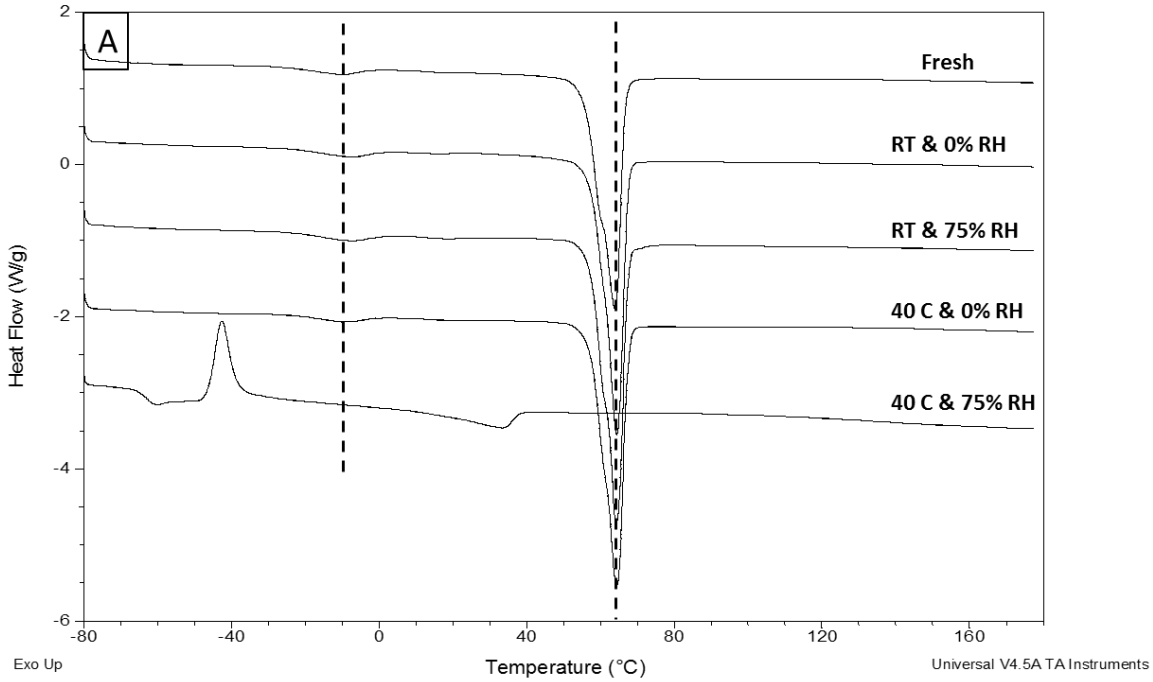

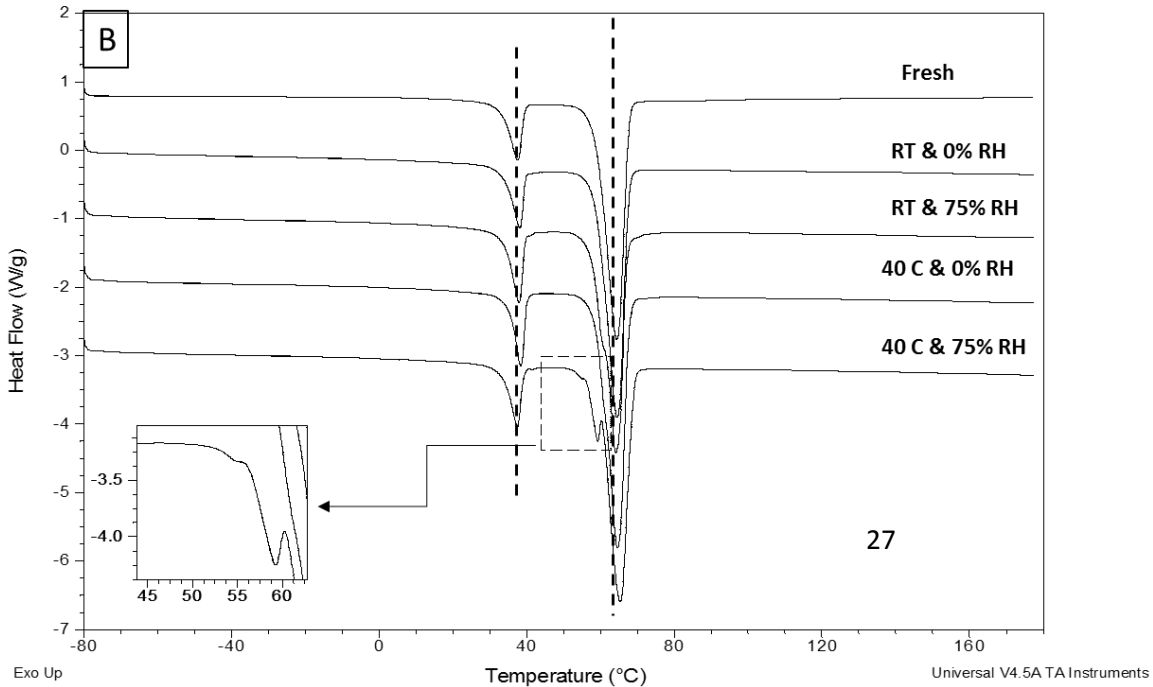

Figure 2. TGA results of (A) 3-month aged CM1 placebo patches and (B) raw materials (with a heating rate of 10˚C/min).

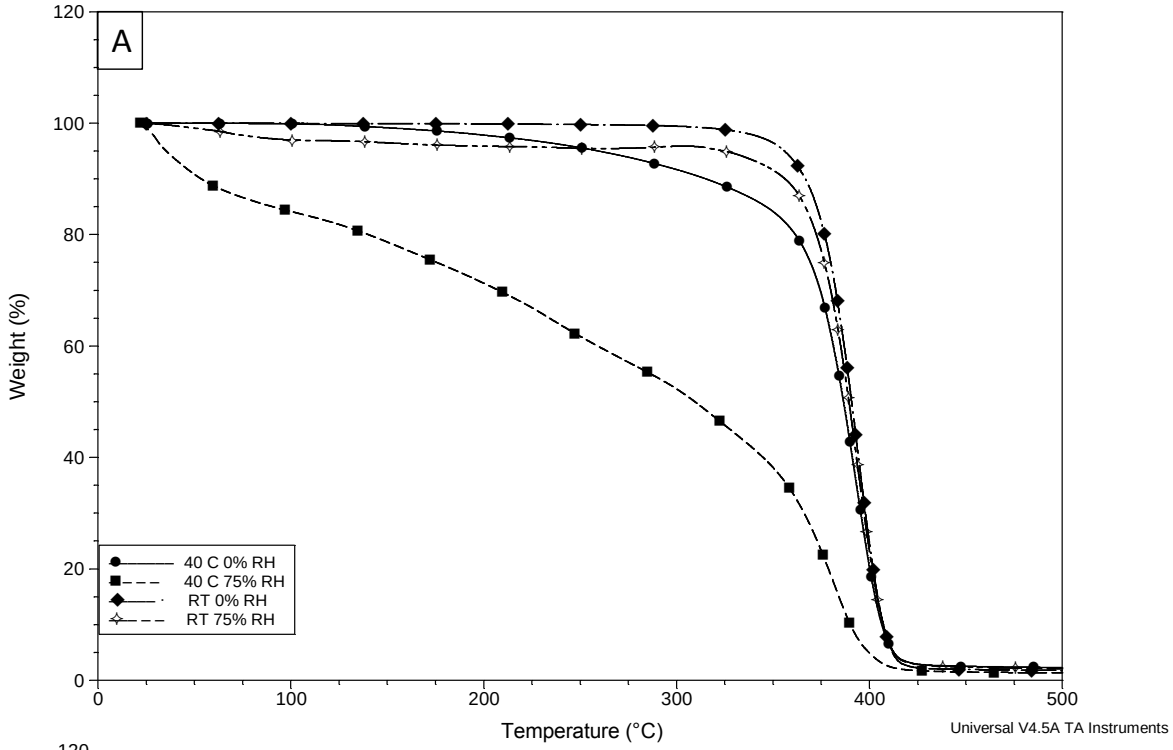

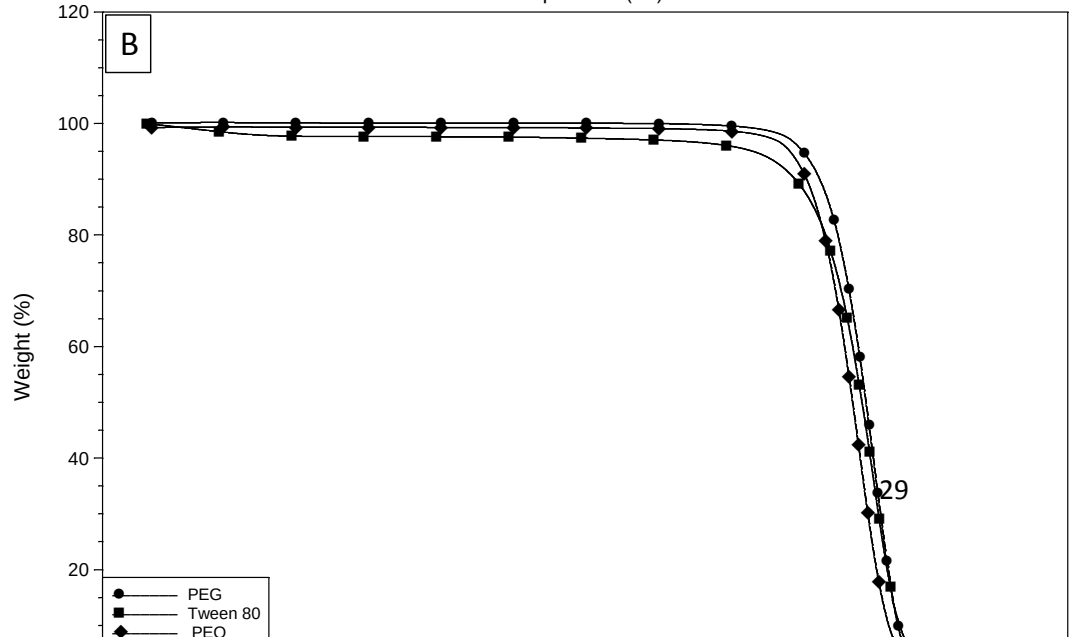

Figure 3. SEM of micro-structural changes of the placebo and 20% drug loaded patches before and after 3-month aging under 40°C/75%RH.

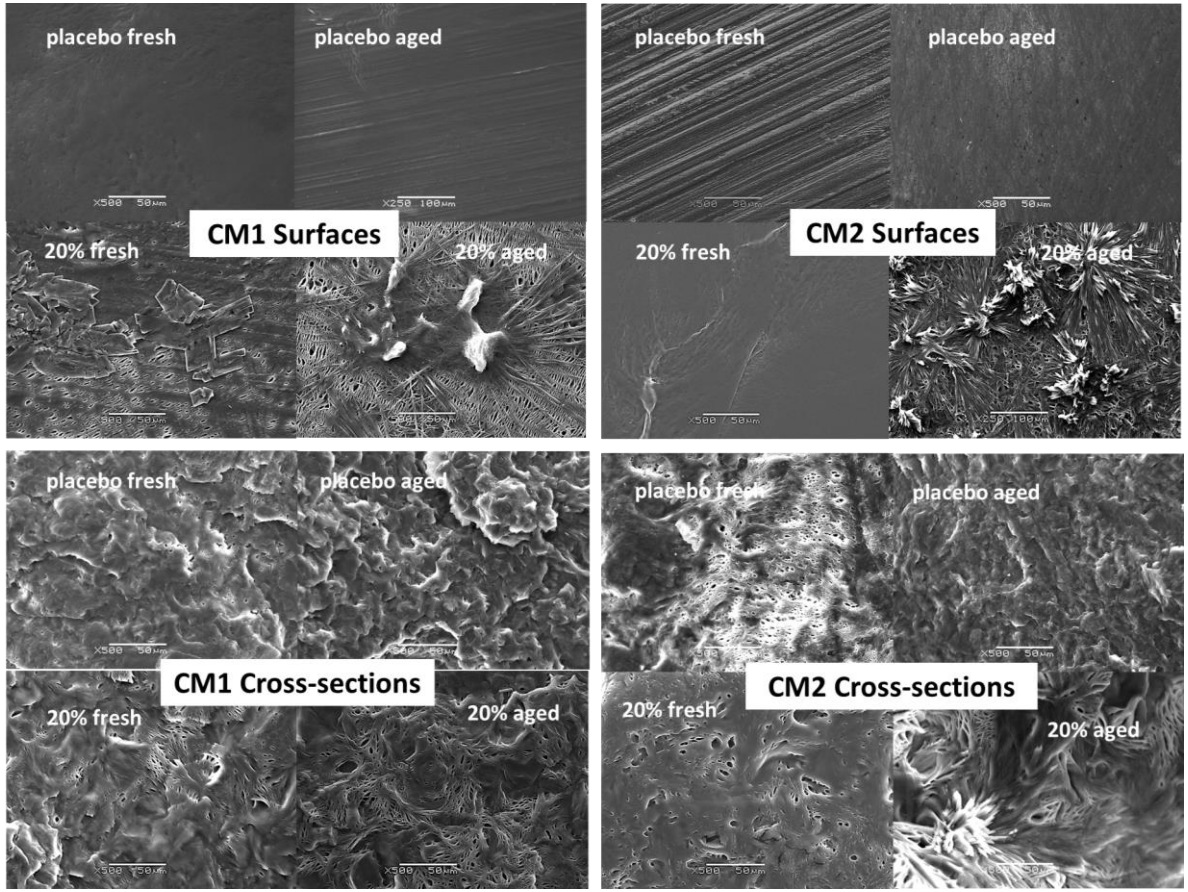

Figure 4. DSC results of 20% drug loaded CM1 patches: (A) PEG/PEO melting and (B) T_g regions; 20% drug loaded CM2 patches: (C) PEG/PEO melting and (D) T_g regions; 30% drug loaded CM1 patches: (E) PEG/PEO melting and (F) T_g regions; and 30% drug loaded CM2 patches: (G) PEG/PEO melting and (H) T_g regions.

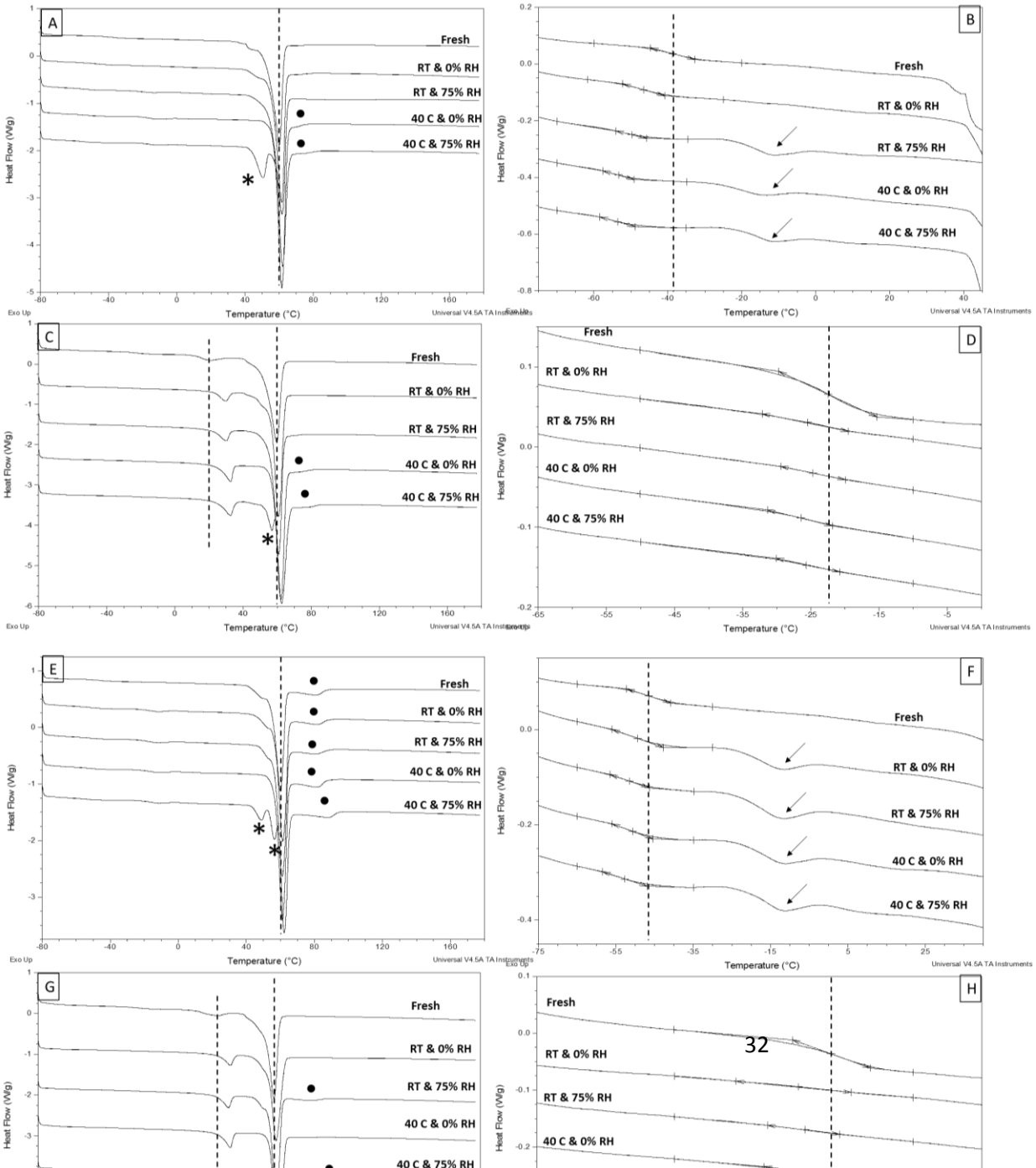

Figure 5. Representative SEM images of different felodipine crystal habits: blocky & plate crystals in (a) in 30% CM1 condition B surface and (b) 30% CM2 condition C interior; needle and plate crystals in (c) 10% CM2 condition C surface and (d) 20% CM1 condition B; fine needle crystals in (e) 30% CM1 condition D surface and (f) interior; and thick needle crystals in (g) 30% CM2 condition D surface and (h) interior.

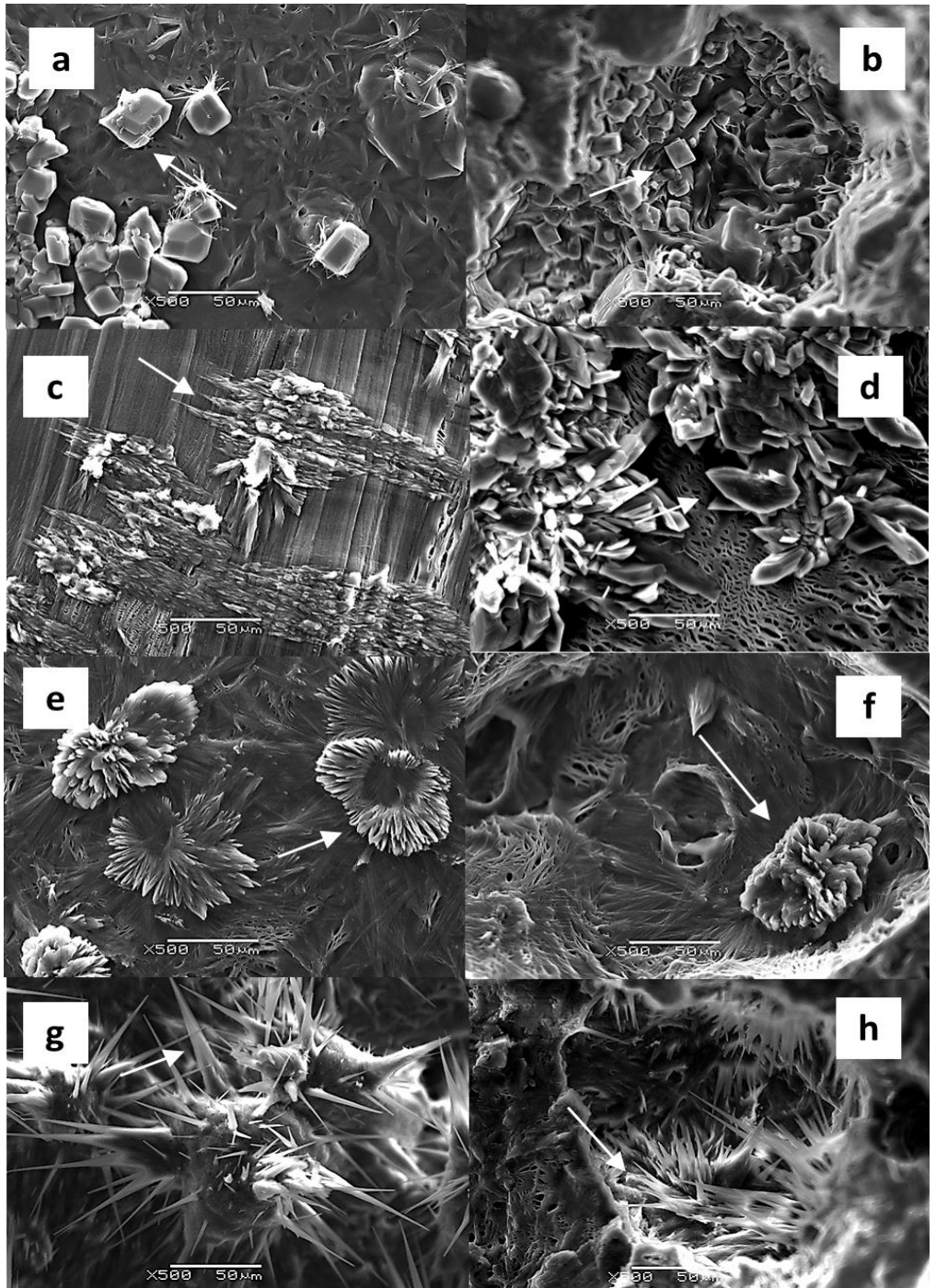

Figure 6. PXRD patterns of 20% w/w drug loaded fresh and 3-month aged (A) CM1 and (B) CM2 patches.

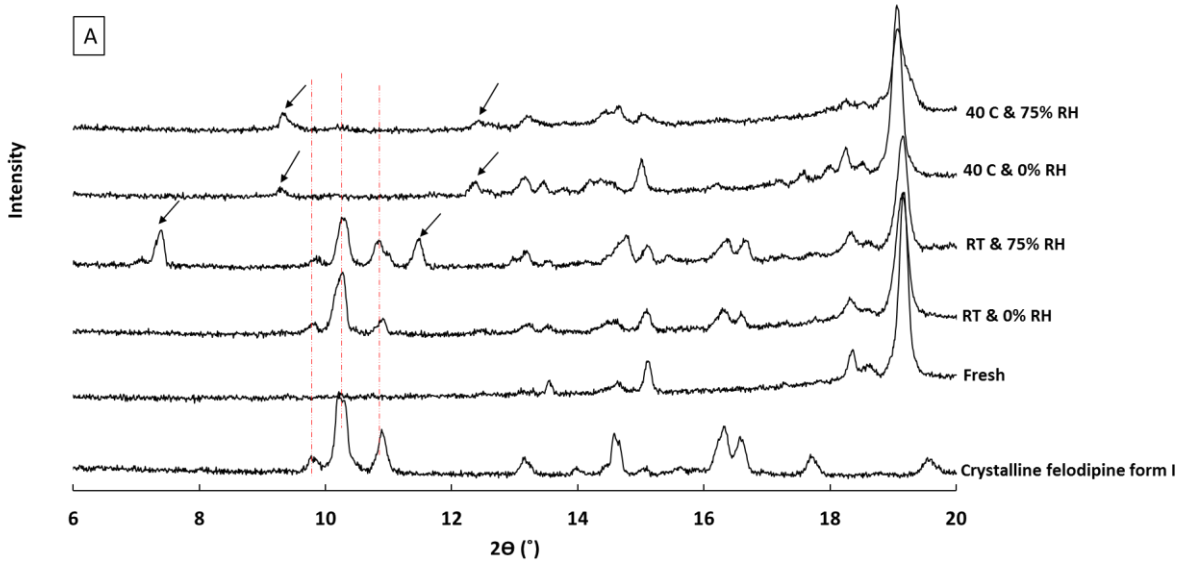

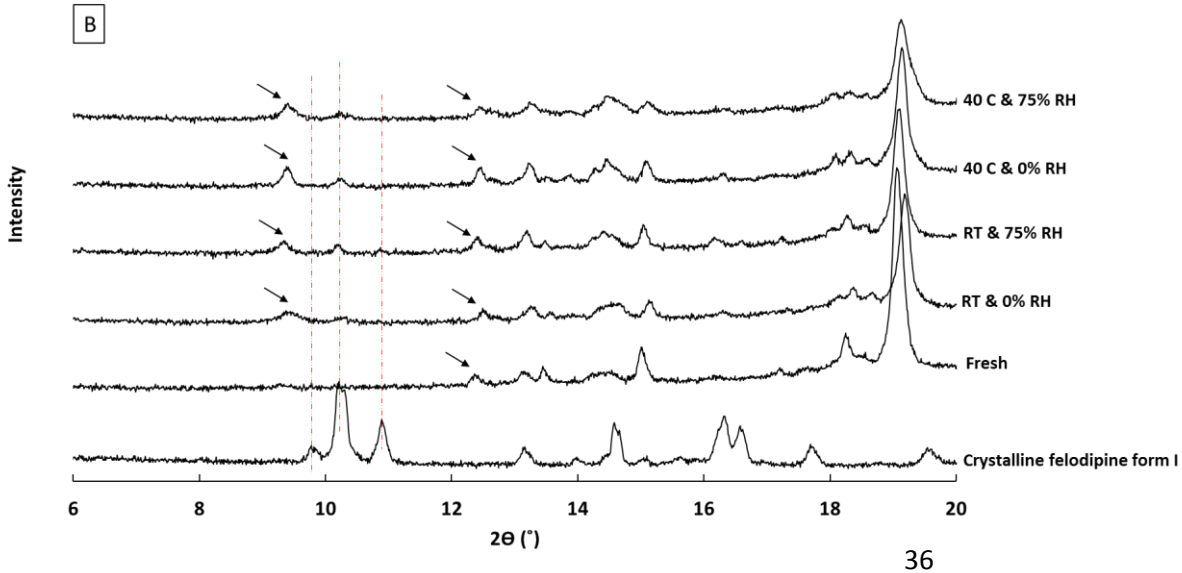

Figure 7. PXRD patterns of 30% w/w drug loaded fresh and 3-month aged (A) CM1 and (B) CM2 patches.

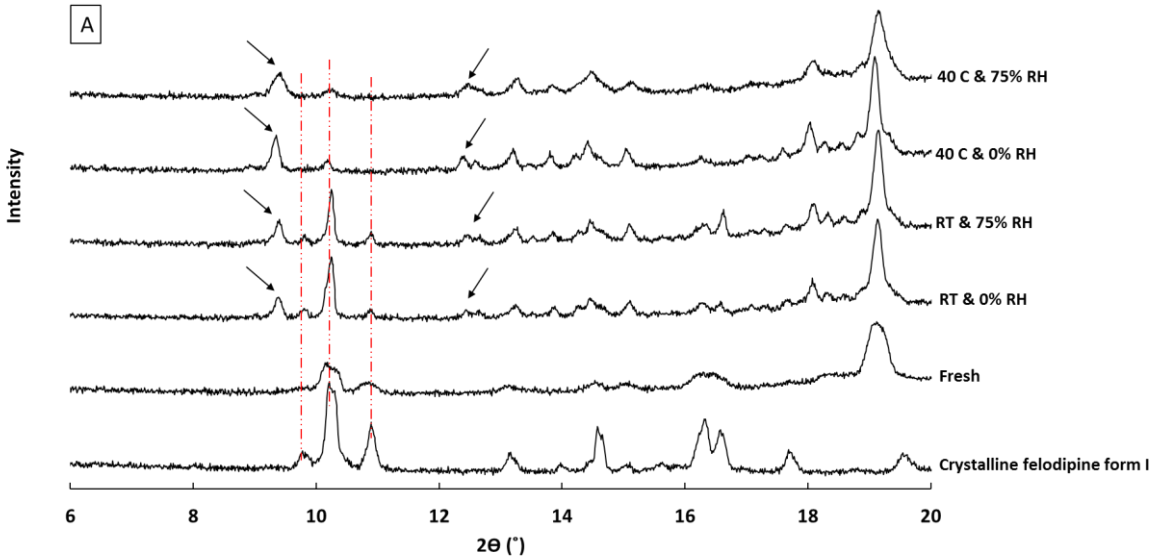

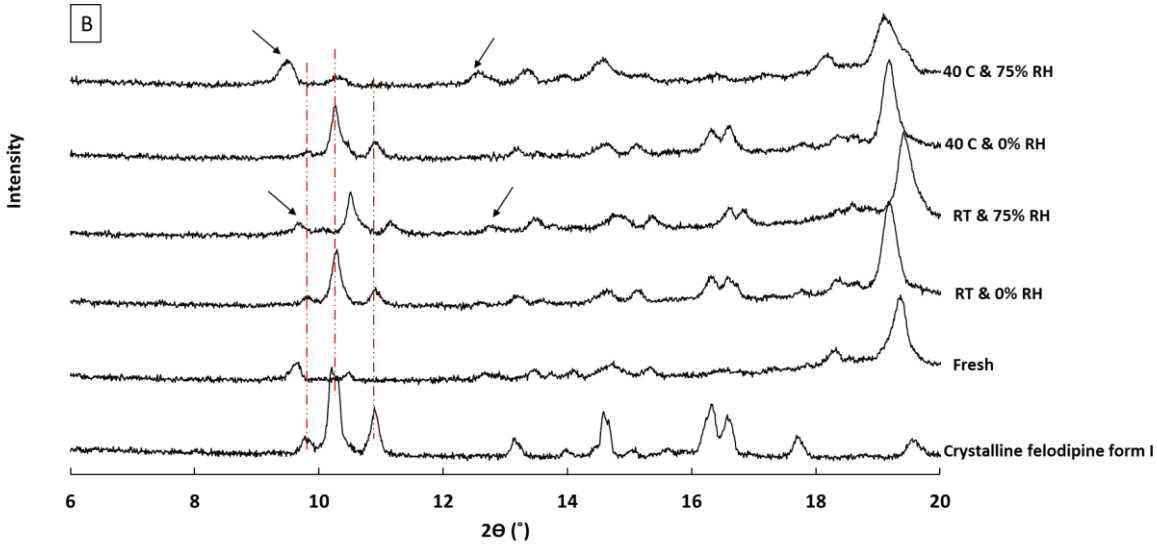

Figure 8. Partial ATR-FTIR spectra of the fresh and aged (A) 20% drug loaded CM1 patches, (B) 20% drug-loaded CM2 patches; (C) 30% drug loaded CM1 patches and (D) 30% drug-loaded CM2 patches.

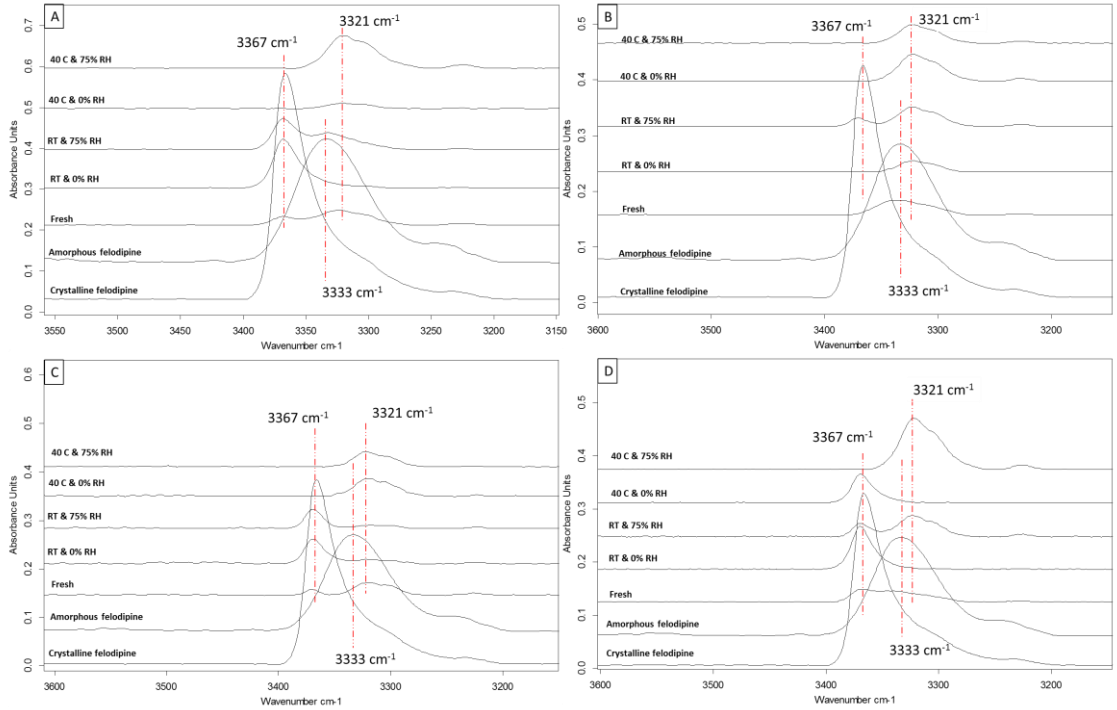

Figure 9 Normalized thermal data of (a) ΔCp and (b) ΔH_f of Tween and TPGS in the fresh and 3-month aged patches. A, B, C and D refer to the 4 different storage conditions.

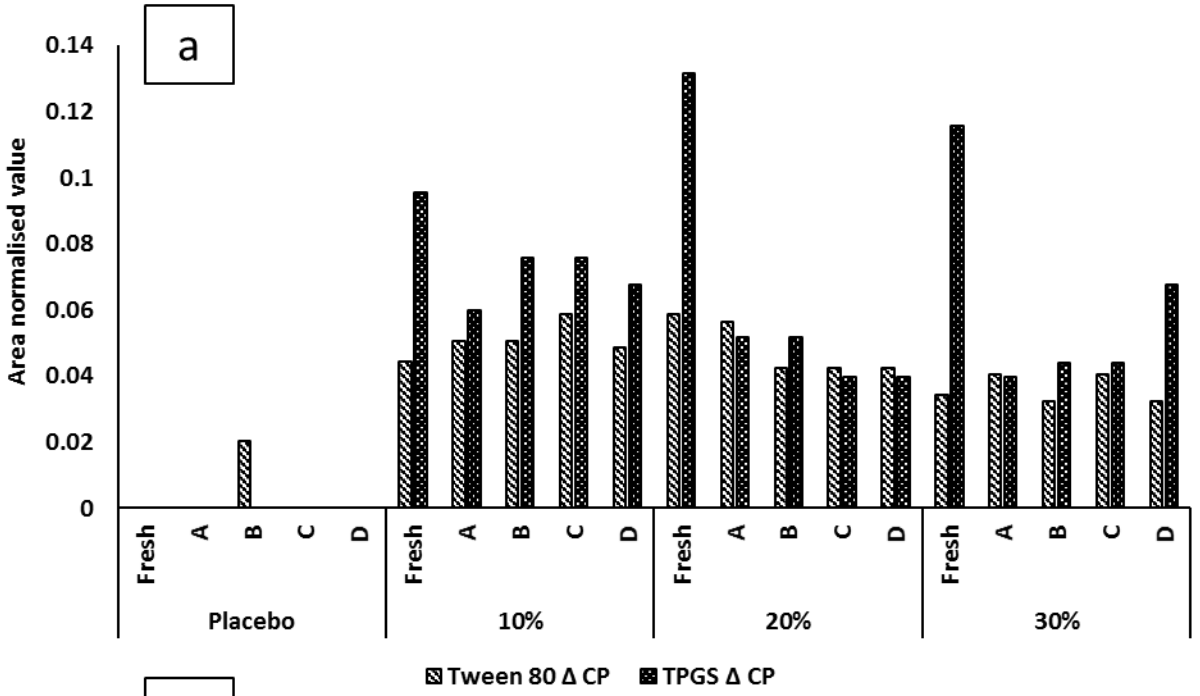

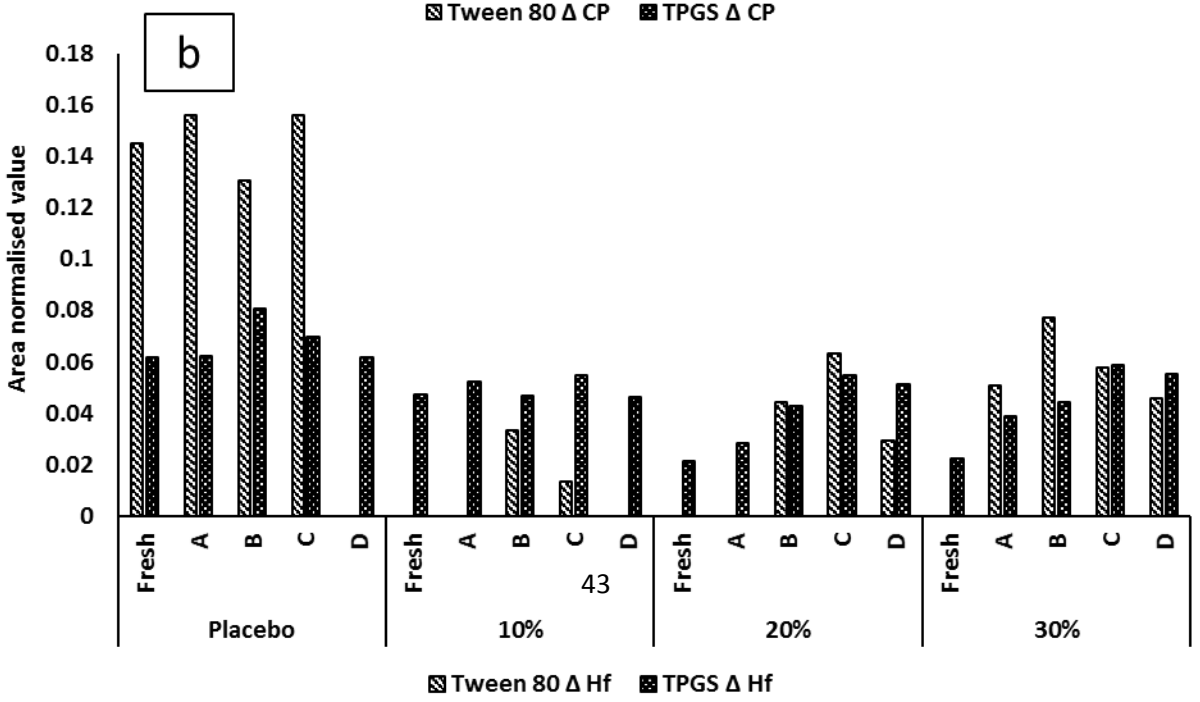

Figure 10. Variances of the thermal values of (a) PEG/PEO and (b) Tween and TPGS during the 3-month of aging under different conditions (note the large differences in scale between the PEG/PEO values and the surfactant values).

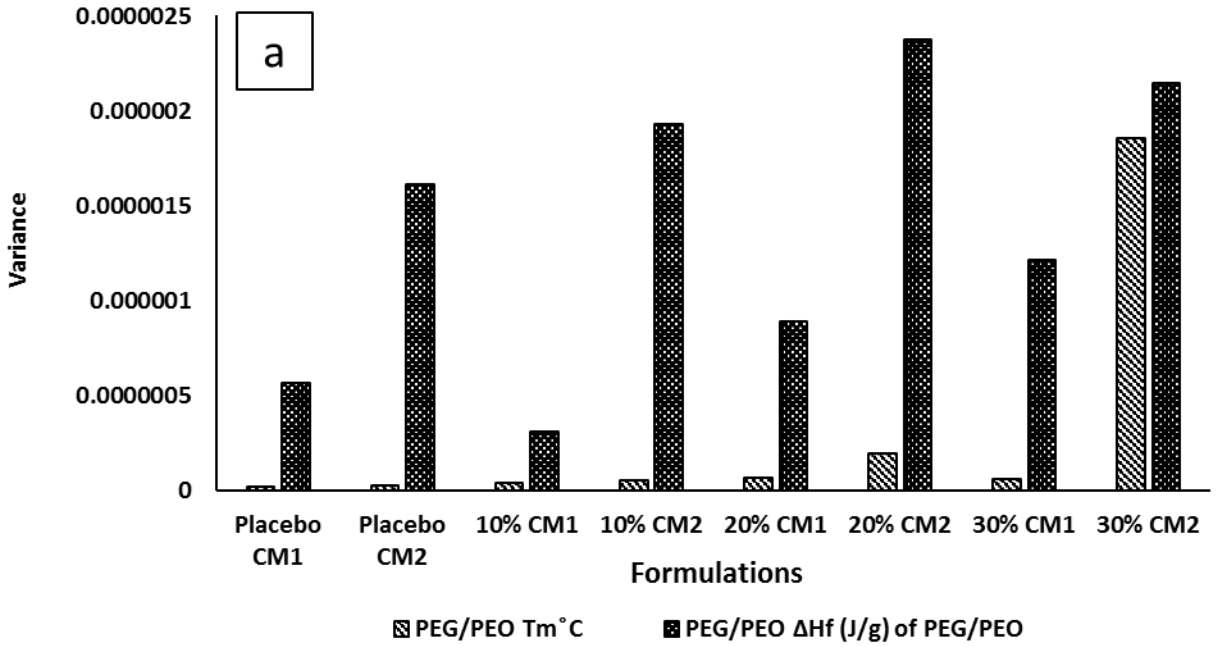

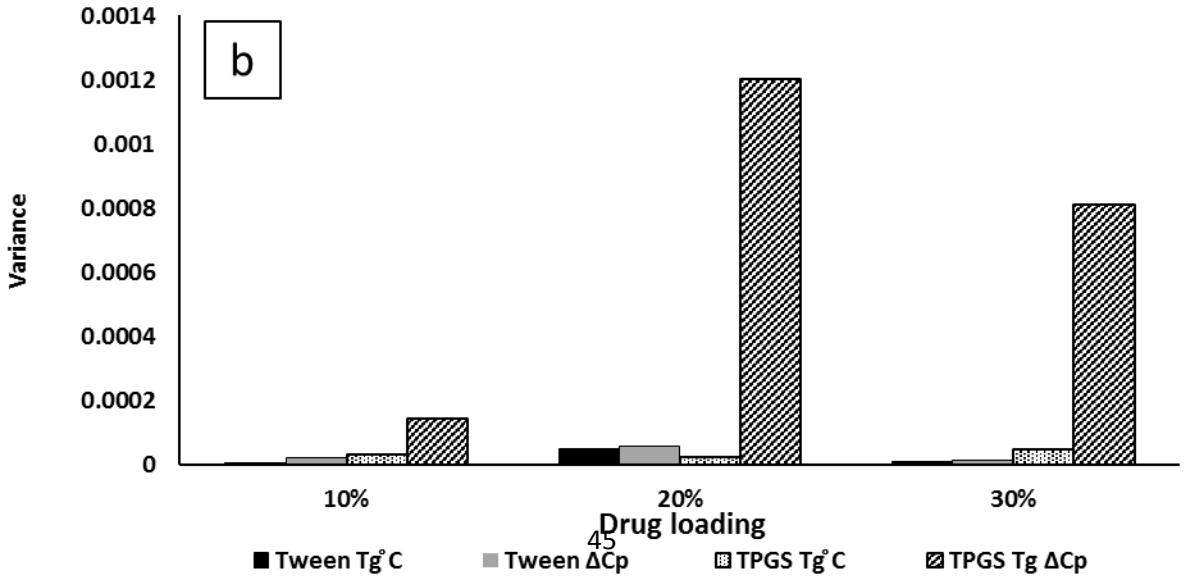

Table 1. Summary of the changes of thermal properties of the aged patches in comparison to the properties of the fresh patches

Formulation		T_g				ΔC_p				PEG/PEO T_m				PEG/PEO ΔH_f				Surfactant T_m				Surfactant ΔH_f			
		A	B	C	D	A	B	C	D	A	B	C	D	A	B	C	D	A	B	C	D	A	B	C	D
CM1 (Tween)	0	↔	↔	↔	↔	↔	↔	↔	↔	↔	↔	↔	*	↑	↑	↑	*	↓	↓	↓	*	↑	↓	↑	*
	10	↔	↔	↔	↔	↔	↔	↔	↔	↑	↑	↑	↔	↔	↔	↑	↔	↔	♦	♦	↔	↔	♦	♦	↔
	20	↓	↓	↓	↓	↔	↓	↓	↓	↑	↔	↑	↑	↔	↔	↑	↔	↔	♦	♦	♦	↔	♦	♦	♦
	30	↓	↓	↓	↓	↔	↔	↑	↔	↑	↑	↑	↑	↑	↑	↑	↔	♦	♦	♦	♦	♦	♦	♦	♦
CM2 (TPGS)	0	↔	↔	↔	↔	↔	↔	↔	↔	↔	↔	↑	↑	↔	↓	↑	↑	↑	↑	↑	↔	↔	↑	↑	↔
	10	↔	↓	↔	↔	↓	↔	↔	↔	↔	↔	↔	↔	↑	↔	↔	↔	↑	↔	↑	↓	↔	↔	↑	↔
	20	↓	↓	↓	↓	↓	↓	↓	↓	↑	↑	↑	↑	↑	↔	↑	↔	↑	↑	↑	↑	↑	↑	↑	↑
	30	↓	↓	↓	↓	↓	↓	↓	↓	↑	↑	↑	↑	↔	↔	↑	↔	↑	↑	↑	↑	↑	↑	↑	↑

(*) stands for the sample liquefied after 3 months storage and not testable
(↑) value increased in comparison to fresh samples
(↓) value decrease in comparison to fresh samples
(↔) value shows no significant change in comparison to fresh samples
(♦) value decreased in comparison to pure Tween 80 (due to undetectable Tween 80 melting peak in the fresh samples)

Table 2. Summary of surface morphology and crystal growth of the 3-month aged HMIM patches obtained by SEM

Drug loading (% w/w)	Formulation	CM1 (with Tween 80)								CM2 (with TPGS)							
	Location	Surface				Cross-section				Surface				Cross-section			
	Ageing condition	A	B	C	D	A	B	C	D	A	B	C	D	A	B	C	D
10	Fresh	-				-				-				-			
	Aged	B	B	B+S	S	-	-	-	-	P	B	P	-	-	-	-	-
20	Fresh	P				-				-				-			
	Aged	P	P	-	S	-	-	-	-	B	B	P	S	-	-	-	S
30	Fresh	B				P+S				-				-			
	Aged	B	B	S	S	S	B+S	S	S	B	B	B	S	B	B	B	S

(S) Spherulitic crystals
(B) Block shaped crystals
(P) Plate crystals
(-) No crystals were detected

Table 3. Crystal polymorphs identification of aged patches determined by PXRD and ATR-FTIR.

	Formulations	CM1				CM2			
Drug loading (% w/w)	Storage conditions	A	B	C	D	A	B	C	D
10	Fresh	-				-			
	Aged	1	1	-	-	-	-	-	-
20	Fresh	-				NF			
	Aged	1	1,2	NF	NF	NF	1,NF	1,NF	1,NF
30	Fresh	1				*			
	Aged	1	1,NF	1,NF	1,NF	1	1	1	NF

(-) No crystalline drug detected
(1) Felodipine polymorphic I
(2) Felodipine polymorphic II
(NF) New polymorphic form that does not match the PXRD and IR data of any polymorphic form reported in the literature
(*) Broad IR peaks and weak PXRD diffraction peak did not allow identification